

METAMORPHISM, COOLING RATES, AND MONAZITE GEOCHRONOLOGY OF THE SOUTHERN ADIRONDACKS¹

by

Lara C. Storm and Frank S. Spear

Department of Earth and Environmental Sciences, Rensselaer Polytechnic Institute, Troy, NY 12180

¹This article accompanies the field trip guide
"Geology and Geochronology of the Southern Adirondacks"

INTRODUCTION

Metamorphism in the Adirondacks has been the subject of investigation for over a century, beginning with the early work of Ebenezer Emmons. As summarized by Bohlen et al. (1985) and Valley et al. (1990), the Adirondack highlands have been characterized by a more-or-less concentric ("bull's eye") pattern of peak-metamorphic isotherms, based largely on re-integrated Fe-Ti oxide and feldspar thermometry (Fig. 1a). Published P-T paths for the central Adirondacks are counter-clockwise with cooling from peak conditions inferred to be nearly isobaric (Bohlen et al., 1985; Spear and Markussen, 1997).

The initial motivation for undertaking petrologic investigation of the southern Adirondacks was two-fold. Firstly, significant outcroppings of high-grade pelitic gneisses (migmatites) occur in the southern and eastern Adirondacks, and rocks of these bulk compositions have not been examined in detail using modern petrologic methods. Secondly, the isotherm pattern (Fig. 1a) indicates that the lowest grade metamorphic rocks (<675 °C) occur in the southern Adirondacks, making this an excellent area to test the validity of the metamorphic "bull's eye". Additionally, previous studies (e.g. Whitney, 1978) report the presence of migmatites in the southern Adirondacks, suggesting that the peak temperatures might be significantly higher than suggested by Fe-Ti oxide and feldspar thermometry.

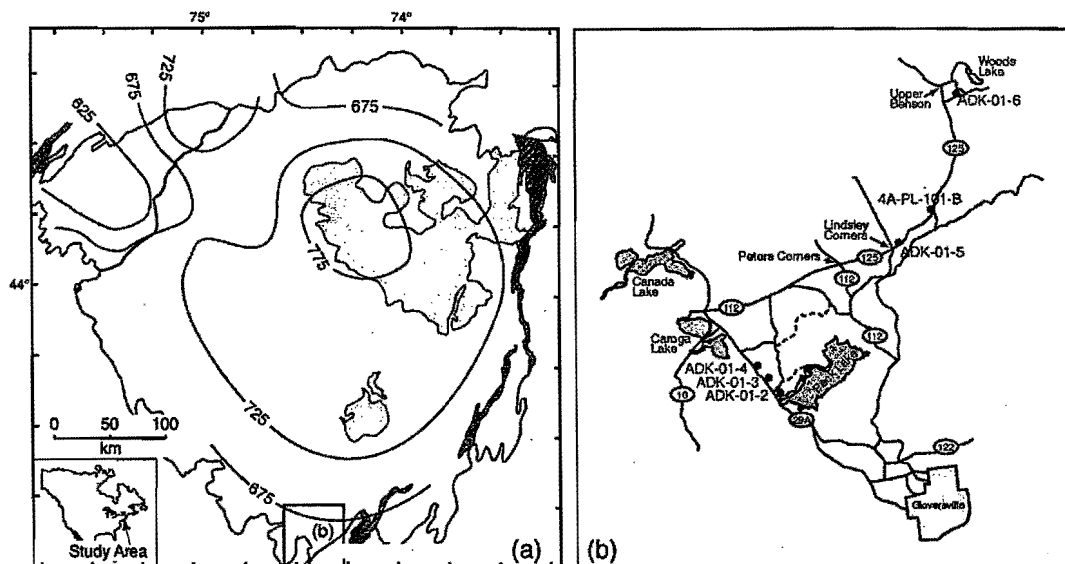


Figure 1. (a) The thermal "bull's eye" of Bohlen et al. (1985) superimposed on a map of the Adirondacks. An enlarged map of area (b) showing roads, locations, and sample numbers.

PETROGRAPHY

Eleven samples from five outcrops in the southern Adirondacks were collected during the winter of 2001 for detailed investigation (see Fig. 1b for localities). An additional sample (4A-PL-101-B) was obtained from J. McLelland. All outcrops examined contain highly foliated aluminous pelitic gneisses and many of the samples are sillimanite-bearing. Migmatites are abundant with the percentage of leucosomes ranging from a few per cent to one-fourth of the outcrop.

The dominant assemblage in the investigated samples includes biotite + quartz + plagioclase + K-feldspar ± garnet ± sillimanite + Fe-Ti oxides ± monazite ± apatite. Melanosomes contain the above assemblage whereas leucosomes are dominated by quartz + plagioclase + K-feldspar. Many leucosomes contain garnet crystals, suggesting leucosome formation by the reaction

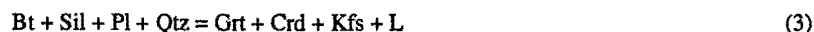


Prograde muscovite (except for retrograde sericite) is not present, indicating that peak P-T conditions were above the muscovite dehydration melting reaction. In addition, late muscovite has been found in only one sample, suggesting that in most samples, all melt that was produced from muscovite dehydration (Rxn. 2) has been expunged from the rock.



The single muscovite-bearing sample (ADK-01-5) displays the unusual texture of muscovite pseudomorphs after sillimanite, in association with quartz. Retrograde progress of reaction 2 is inferred to be the origin of this late muscovite.

Cordierite and orthopyroxene were not observed in any samples (and, to our knowledge have not been reported in metapelitic rocks from the southern Adirondacks), restricting P-T conditions to lie below the reactions



and



These petrographic observations are consistent with the migmatites having formed from dehydration melting. During dehydration melting the activity of water ($a_{\text{H}_2\text{O}}$) is buffered by the solid + liquid assemblage to values less than $\text{PH}_2\text{O} = \text{P}_{\text{total}}$, consistent with the general observation of low $a_{\text{H}_2\text{O}}$ in Adirondack granulites. Thus, in the absence of large scale fluid infiltration (e.g. Valley et al., 1990), experimental and calculated dehydration melting reactions place broad limits on the peak P-T conditions of the southern Adirondacks (Fig. 2).

GARNET ZONING AND REACTION HISTORY

Garnet crystals are resorbed and display chemical zoning that reflects a multiple-stage growth history (Fig. 3). Garnet cores are relatively unzoned in major elements ($X_{\text{prp}} = 0.053$, $X_{\text{alm}} = 0.330$, $X_{\text{sps}} = 0.0095$, $X_{\text{grs}} = 0.017$). Towards the garnet rim, Fe and Fe/(Fe+Mg) increase whereas Mg decreases, consistent with diffusion controlled zoning produced during melt crystallization by the retrograde progress of reaction 1 during cooling.

Grossular content is higher near garnet rims and does not display diffusive zoning as seen in Fe and Mg. The higher grossular content on the rims can be explained by the following reaction sequence. Progress of the muscovite melting reaction (Rxn. 2) exhausted the southern Adirondack rocks of all muscovite and altered the modes and compositions of plagioclase, potassium feldspar, and sillimanite. Reaction 2 (muscovite dehydration melting) proceeds over a relatively small temperature interval until all muscovite is exhausted. Plagioclase involved in this reaction becomes more anorthitic as melting proceeds, as does coexisting melt. Garnet is not involved in Reaction 2, so at the beginning of the reaction, garnet will be in equilibrium with a plagioclase that is more albitic than at the end of the reaction. When garnet growth resumes by Reaction 1, newly grown garnet will be more Ca-rich,

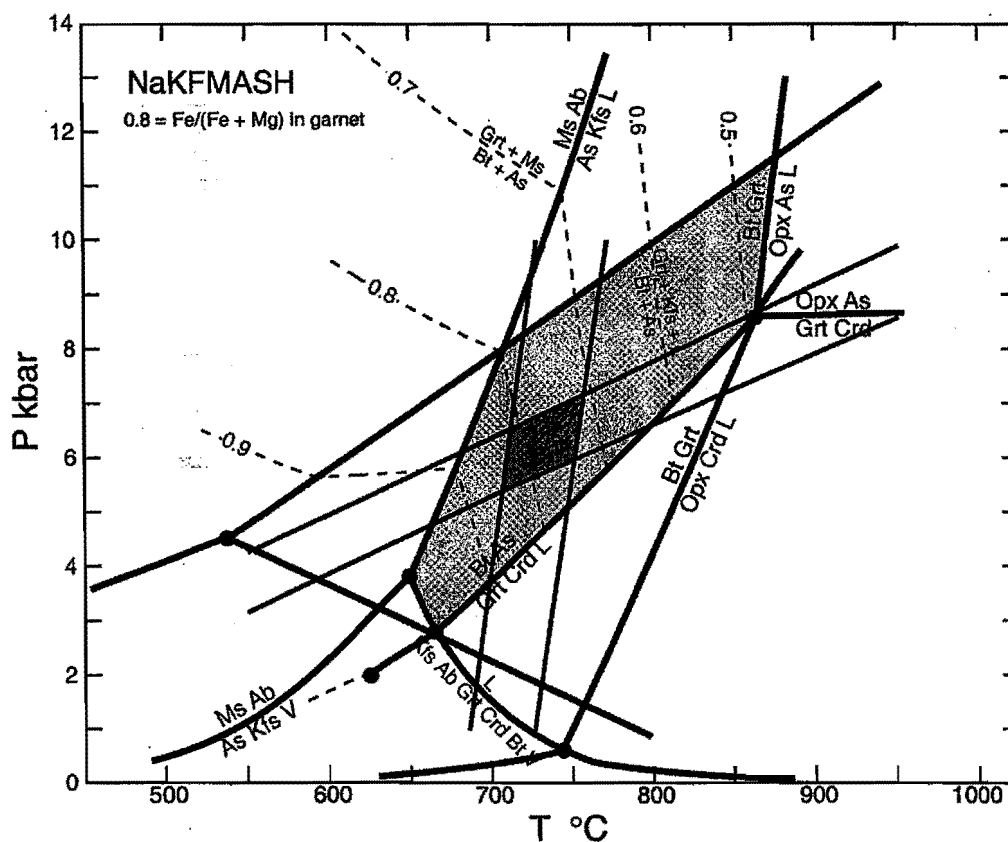


Figure 2. A P-T diagram showing the narrow P-T region to which the peak metamorphic conditions are restricted. The boundaries of the region are determined by the presence of melt and the absence of cordierite or orthopyroxene in metapelitic rocks. The darker parallelogram shows the peak P-T conditions defined by geothermobarometry.

reflecting equilibrium with the more anorthitic plagioclase, producing the observed discontinuous increase in grossular content (e.g. Spear and Kohn, 1996). Therefore, the high-calcium rims are thought to represent the melt-produced garnet, and lower Ca-cores are garnet produced by sub-solidus reactions.

THERMOBAROMETRY

There is clear evidence in the southern Adirondack metapelites for both retrograde Fe-Mg exchange reactions (ReERS) and retrograde net transfer reactions (ReNTRs), making recovery of peak metamorphic compositions for use in thermobarometry difficult (e.g. Kohn and Spear, 2000). ReNTRs and ReERS produce different compositional changes in garnet and biotite. Fe-Mg exchange results in garnet increasing and biotite decreasing their Fe/(Fe+Mg) at the reaction interface as temperature decreases. Reaction 1r results in both garnet and biotite increasing their Fe/(Fe+Mg) as temperature decreases. Temperatures calculated using garnet-biotite pairs that have been affected by ReNTRs and ReERS can be higher, lower, or fortuitously the same as the peak temperature.

Retrograde Fe-Mg exchange has clearly affected biotite inclusions within garnet (Fig. 4). The zoning observed at garnet rims (Fig. 3), in addition to the resorbed shape, suggests retrograde progress of reaction 1:



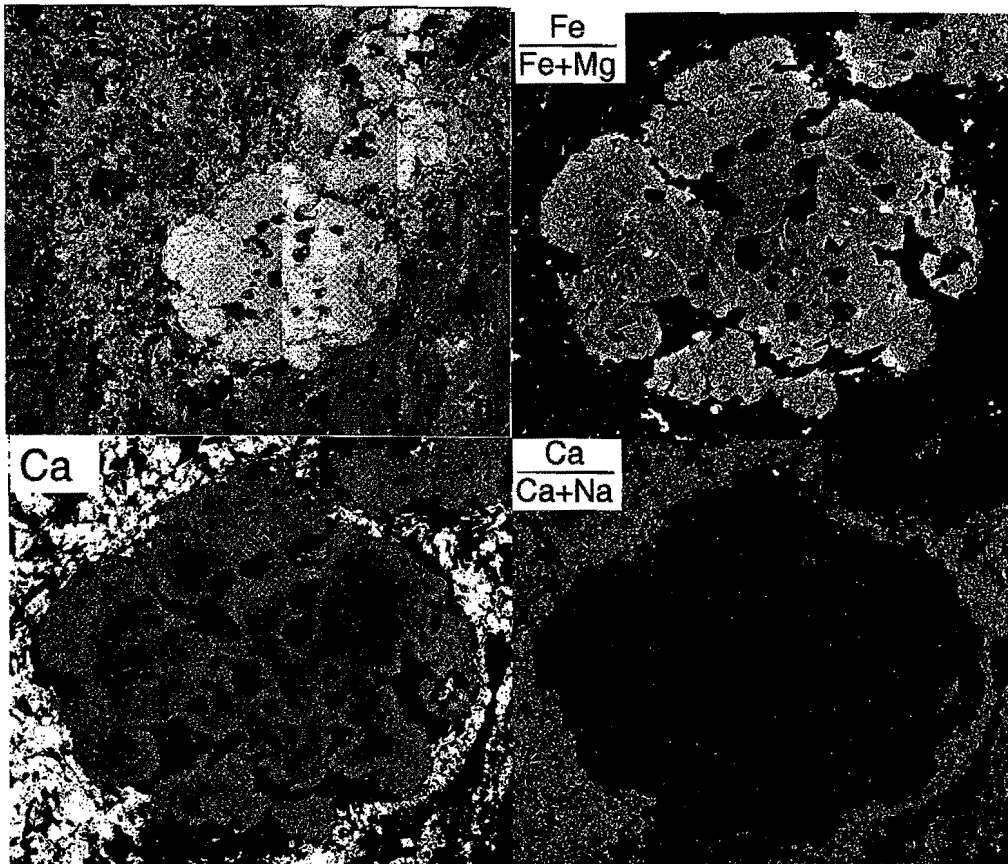


Figure 3. X-ray maps of a garnet from sample 4A-PL-101-B. This garnet displays rims with higher Ca and Fe/(Fe+Mg), which is interpreted to be garnet produced during dehydration melting. The garnet also shows a textural change across the high-Ca rim where inclusions are smaller and more numerous. The matrix plagioclase is slightly zoned in Ca/(Ca+Na).

which occurs as melt crystallizes in leucosomes. ReNTRs such as reaction 1r are ubiquitous in migmatites because the H₂O needed to rehydrate the solid phases (in this case biotite) is dissolved in the liquid and exsolves as the liquid crystallizes. The presence of muscovite pseudomorphs after sillimanite further suggests retrograde progress of reaction 2.

The approach taken here is to use the composition of the garnet core well away from biotite inclusions with the composition of matrix biotite away from the garnet rim. Although the matrix biotites may have been affected by reaction 1r (which would yield a temperature higher than the peak T), the extent of reaction 1r is not large, as evidenced by the absence of Mn zoning on the rim. Peak pressures were calculated using the high-Ca rim with matrix plagioclase.

Results of thermobarometry calculations are summarized in Figure 2. The garnet-biotite thermometer of Patiño Douce et al (1993) was used because it takes into consideration the Ti-content of biotite. The GASP barometer of Hodges and Crowley (1985) was used to determine minimum and maximum pressures (high-Ca garnet with low-Ca plagioclase and vice-versa) which define a narrow pressure range. Only curves representing the range of conditions believed to be representative of the peak conditions are shown. The peak temperature is approximately 710-740 °C

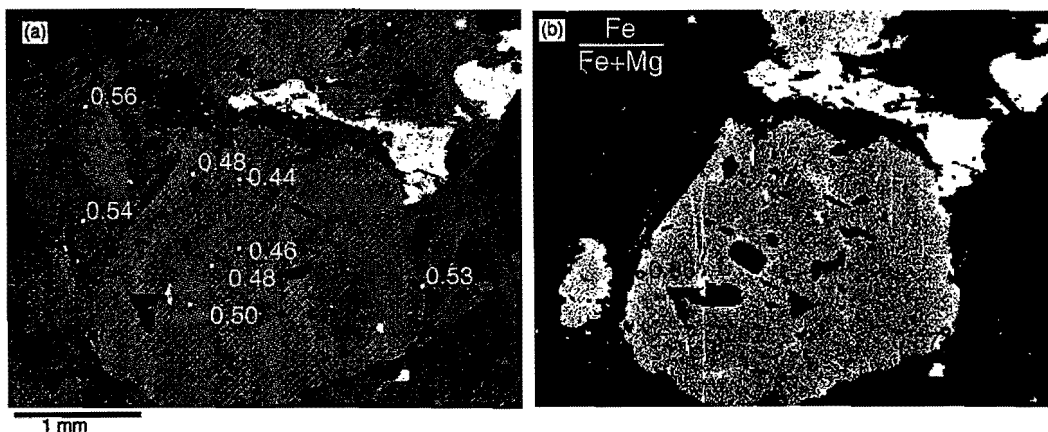


Figure 4. (a) Backscatter image of garnet from sample ADK-01-5, which contains a plethora of variably sized biotite inclusions. Numbers are Fe-Mg ratios for different biotite grains. Note that Fe/(Fe+Mg) of biotite within garnet is a function of the size of the inclusion. (b) X-ray map showing Fe/(Fe+Mg) in garnet. Numbers are measured Fe/(Fe+Mg). Note high-Fe rims on garnet and high halos around biotite inclusions. Cooling rate calculations performed on this garnet yield a cooling rate of around 2 to 5 °C/Ma (see Figure 6).

at 6 kbar, and is consistent with the constraints imposed by mineral assemblages. It should be noted that this temperature is significantly higher than the < 675 °C predicted by the bull's eye pattern (Fig. 1a), and suggests that the peak metamorphic temperatures in the Adirondacks may not be concentric around the anorthosite (see also Whitney, 1978). It may also be significant that the peak pressure of 6 kbar is lower than that recorded in the central highlands (e.g. Spear and Markussen, 1997), suggesting that there may be a gradient in peak pressure from north to south.

COOLING RATES FROM GARNET-BIOTITE FE-MG EXCHANGE

Spear and Parrish (1996) present a method that utilizes the exchange of Fe and Mg between biotite inclusions within garnet and garnet host to estimate post-peak cooling rates. As seen in Figure 4, there is a correlation between the Fe/(Fe+Mg) of biotite inclusions and size of the inclusion. Minor zoning of Fe/(Fe+Mg) is observed in garnet around biotite inclusions, but the magnitude of this zoning prohibits precise constraints on cooling rates. This method circumvents this limitation by using the composition of the biotite as a monitor of the total flux of Fe and

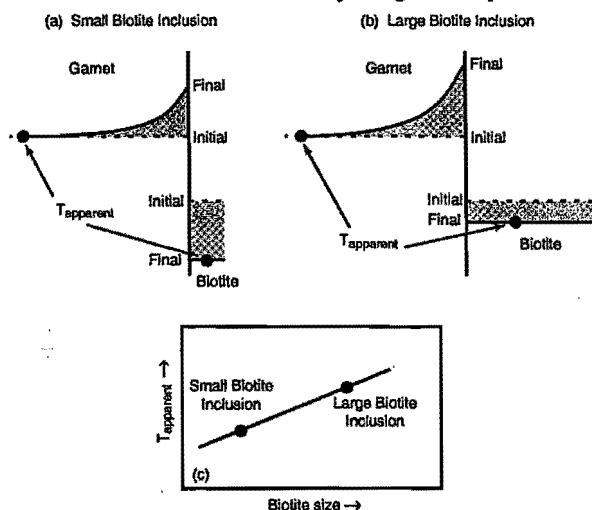


Figure 5. An illustration of the relationship between biotite inclusion size and Fe/Mg. (a) The smaller biotite inclusion experiences a greater increase in Mg than the larger biotite (b) because for a fixed diffusive flux there is a smaller volume over which to distribute the incoming Mg. (c) A plot of the apparent T calculated from garnet-biotite thermometry versus log of biotite size showing the predicted linear relationship.

Mg between biotite and garnet. Because diffusivity of Fe and Mg in biotite is rapid relative to garnet, biotite inclusions are generally homogeneous. Application of this method is simple. An apparent temperature is calculated using the composition of the biotite inclusion and the composition of the garnet core away from the inclusion (so that it has not been affected by diffusion; see Fig. 5). The apparent temperature is plotted against a measure of biotite size, and cooling rate isopleths are estimated from model simulations of the diffusive exchange between garnet and biotite at different cooling rates. A large uncertainty in application of the method stems from the difficulty in obtaining an accurate measure of the volume of the biotite inclusion. Firstly, the shape of the crystals is irregular, and it is not usually apparent what geometry should be assumed. Secondly, there is no certainty that the thin section cut goes through the maximum dimension of the biotite so that the true size can be viewed in thin section. Spear and Parrish (1996) explored a number of ways of measuring the biotite size including the use of area percents and linear measurements coupled with cylindrical and spherical geometries. They concluded that the uncertainties were similar with each method and gave similar cooling rates (provided that the model diffusion calculations were plotted each with the same measure of size). A simple linear measure of biotite diameter along the cleavage trace proved to be the easiest way to apply this approach.

Results of the application of this approach to one sample from the southern Adirondacks are presented in Figure 6. Although there is some scatter in the data, the plot reveals the cooling rate to be between 1 and 10 °C/Ma. This is a relatively slow cooling rate and is consistent with the post-peak cooling rate inferred by Mezger et al. (1989, 1991) of about 5 °C/Ma based on U/Pb geochronology of the minerals garnet, biotite, hornblende, sphene, monazite, and rutile.

A slow cooling rate is also consistent with the inferred P-T path of nearly isobaric cooling. The peak P-T conditions of around 725 °C and 6 kbars reflect an elevated geotherm (i.e. higher than steady state) at the peak of metamorphism. Thermal decay of such an elevated geotherm back to a steady state condition by thermal conduction over the length scale of the entire crust (40-60 km) occurs over a time scale ($t = x^2/K$) of 50-100 Ma, requiring 100-200 million years to cool from the peak temperature of approximately 725 °C to the steady state value of approximately 525 °C at 0.6 GPa. This simple cooling model of 200 °C in 100-200 million years yields an average cooling rate of approximately or 1-2 °C/Ma.

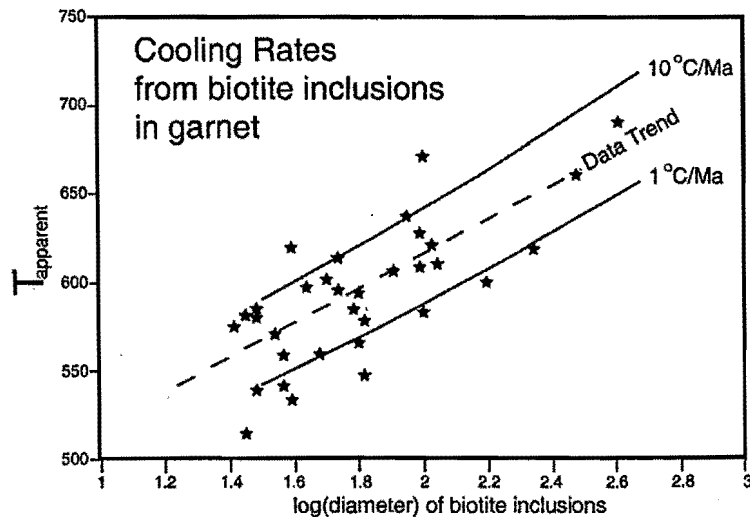


Figure 6. A plot of apparent temperature vs. log of the biotite inclusion diameter for sample ADK-01-5 (Fig. 4). Apparent temperatures are obtained using garnet-biotite thermometry (inclusion + garnet core composition). The cooling rate isopleths were calculated using a finite-difference diffusion program. The plot reveals a cooling rate between 1 and 10 °C/Ma.

GEOCHRONOLOGY

Introduction

Chemical dating using the electron microprobe is a texture-sensitive approach that enables ages of discrete chemical domains within monazite to be determined. Under optimal conditions, Pb can be measured on the electron microprobe to a precision of ± 25 ppm (1 σ s.e.). In Proterozoic monazites such as are found in the southern Adirondacks, the Pb content is typically greater than 2000 ppm, enabling ages to be determined to a precision on the order of 1% (i.e. 10 Ma out of 1000). In practice, multiple analyses of the same material yield a precision on the order of ± 20 -30 Ma (1 σ s.e.), but this age resolution is sufficient to distinguish various phases of Grenville metamorphism.

Monazite petrography, chemical zoning, and ages

Monazite is nearly ubiquitous in the migmatitic gneisses of the southern Adirondacks. It occurs as inclusions in all the major phases and within the matrix. Monazite is complexly zoned, suggesting that it might record several episodes of growth.

Monazite inclusions within other phases. Monazite inclusions are found in garnet in at least one sample from every outcrop (Fig. 1b). Several monazite crystals in this textural setting are rounded with compositional truncations that can be seen in BSE images (Fig. 7). X-ray maps reveal chemical zoning characterized by high Y values separated by a low-Y region, suggesting a multiple-stage growth.

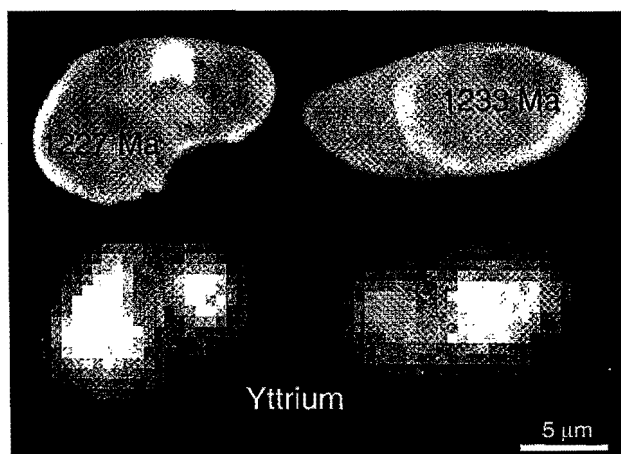


Figure 7. Monazites from sample ADK-01-2 showing what appear to be detrital cores that give ages of around 1230 Ma. These monazites occur as inclusions in garnet and range from about 5 to 10 microns in diameter. The X-ray maps show that the old cores have a higher concentration of Y. The youngest ages given by monazites included within garnet (not shown) are Ottawaan.

arranged with oldest in the cores and youngest on the rims. Furthermore, the age domains are usually chemically distinct. The oldest group (1165-1185 Ma) occurs only in the cores of monazite crystals. These ages correspond to either the waning stages of the Elzevirian orogeny (1300-1180 Ma), or the earliest stages of the intrusion of the AMCG suite (1160-1120). The 1125 Ma age is found in the chemically distinct core of a partially included monazite (Fig. 8). It is not possible at this time to ascertain whether this monazite formed during the waning stage of the AMCG suite intrusion, or during the initial stage of the Ottawaan orogeny (1090-1045 Ma). Near the rims of several

Ages determined from the CHIME method yield 1227 - 1233 ± 10 Ma for the high-Y parts. These are some of the oldest ages encountered in the southern Adirondack monazites and represent an Elzevirian event. The age of the sedimentary protolith of the southern Adirondack paragneisses is not known, and it may be that these monazites pre-date sedimentation. We make the tentative suggestion that these are detrital relics.

Partially included and matrix monazites. Several monazites examined in this study are embedded in the outer, melt-produced rims of garnet (Fig. 8 and 9). Others are in the rock matrix. Zoning in all of these monazites is complex (Figs. 8-10) and indicates several growth phases. The similarities in zoning and overlap in ages indicates that the partially included monazites were in equilibrium with the matrix throughout the metamorphic history.

Several groups of ages are recorded in these monazites (Figs. 8-11), including 1165-1185 Ma, 1125 Ma, 1088-1112 Ma, 1028-1048 Ma, 923 Ma, and 386 Ma. In general, the ages are

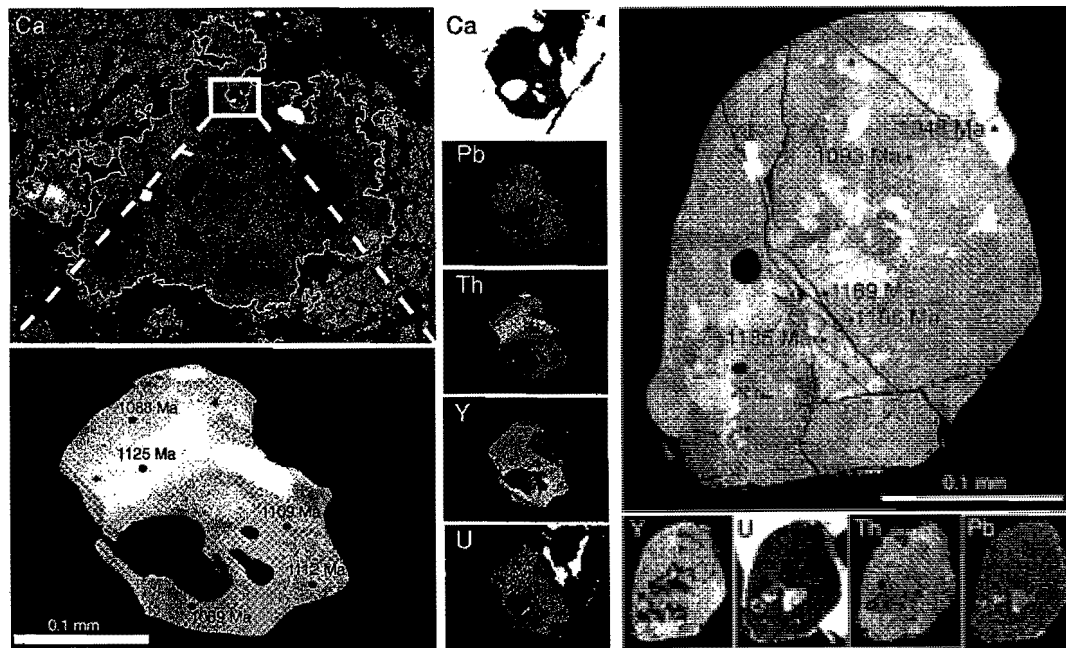


Figure 8. Garnet and monazite from sample ADK-01-4. The garnet has a high-Ca, melt-generated rim. Monazite is embedded (not included) within the garnet. The age distribution (1125-1088 Ma) corresponds to chemical zoning in monazite.

Figure 9. A partially included monazite grain from sample ADK-01-2 displaying complex patchy zoning of Y, U, Th, and Pb. This monazite appears to have three age populations at 1165-1185 Ma, 1093 Ma, and 1048 Ma.

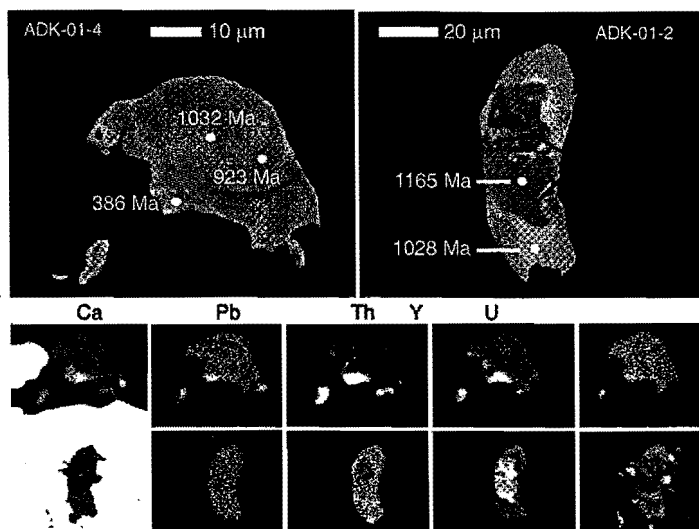


Figure 10. Top panels: BSE images of matrix monazite grains from samples ADK-01-4 and ADK-01-2 showing CHIME ages. Bottom panels: X-ray maps showing chemical zoning in the same grains. Age distribution correlates well with observed zoning patterns. Note the Acadian rim on the monazite from sample ADK-01-4.

monazites are ages of 1112-1088, which correspond to the early stages of the Ottawa orogeny, and possibly represent monazite growth during prograde metamorphism of the pelite. Another suite of ages ranging from 1028-1048 Ma occurs on the monazite rims. The fact that these ages occur on the rims of rocks that had undergone partial melting suggests that they may have formed during melt crystallization. If so, these ages represent the waning stages of the Ottawa orogeny. The 923 Ma age (Fig. 10) may reflect monazite growth associated with the Cathead Mountain dike swarm, which is dated at 935 ± 9 Ma. (McLelland et al., 2001).

A few matrix monazites yielded Paleozoic ages of approximately 400 Ma on their outermost rims (e.g. Fig. 10). The chemistry of these monazite rims is distinct from the rest of the grain and is readily observable with BSE or chemical mapping. The significance of monazite growth at these times is not entirely clear. The inferred thermal history of the Adirondacks predicts that these rocks should not have been hotter than approximately 400 °C, so it is not reasonable that prograde metamorphic reactions were responsible for this growth. The most likely interpretation is that these bits of monazite were deposited from hydrothermal fluids. The correlation of the measured ages with the Acadian metamorphic events to the east may not be coincidental. It is suggested that hydrothermal fluids expelled from rocks to the east by tectonic loading may have been the agent of monazite formation during the Paleozoic.

Allanite geochronology

Monazite crystals from one sample (ADK-01-3) display thin rims of allanite (Fig. 11). This sample exhibits sericite alteration of K-feldspar and minor chloritization of biotite. The allanite is unusually Th-rich, probably because the monazite from which it was formed was Th-rich.

Chemical dating of three allanite rim spots yields ages of 353, 155, and 144 Ma. It is suspected that the 353 Ma age may be a mixed age combining the Proterozoic core and Jurassic rim. Jurassic ages are surprising from the southern Adirondacks, and their significance is not entirely clear. During prograde metamorphism, allanite replaces monazite in the biotite zone ($T \sim 300-350$ °C; Wing et al., 1999). Apatite fission tracks from the Adirondacks (closure temperature of 100-120 °C) record ages that are slightly younger (100-125 Ma; Roden-Tice et al., 2000), so it is clear that the rocks could not have been very hot (or deep) when the allanite formed. The cause of the allanite

formation is even more perplexing. The continent was undergoing rifting at this time and allanite must be the product of hydrothermal alteration. Its formation is likely to have been caused by the same fluids that caused sericitization and chloritization. North-south trending normal faults are prevalent in this area, and it is possible that hydrothermal fluids gained access to moderate crustal levels as a consequence of this faulting.

Cooling history

Figure 12 shows the inferred thermal history of the southern Adirondacks based on these and published data. The temperature corresponding to the oldest monazite ages (1220-1230 Ma – detrital?) is unconstrained. Ages corresponding to intrusion of the AMCG suite (1160-1120 Ma) may reflect early contact metamorphism or hydrothermal activity associated with plutonism. Ages in the range 1088-1112 Ma likely reflect monazite growth during prograde Ottawa metamorphism and ages in the range 1028-1048 Ma corresponds to monazite

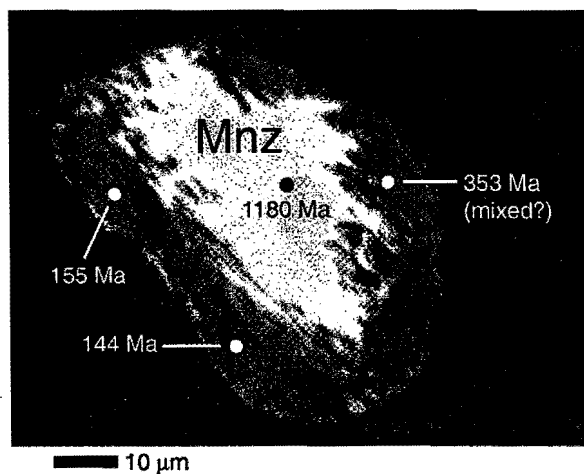


Figure 11. A Proterozoic monazite from sample ADK-01-3 displaying alteration rims of allanite that were formed during the late Jurassic.

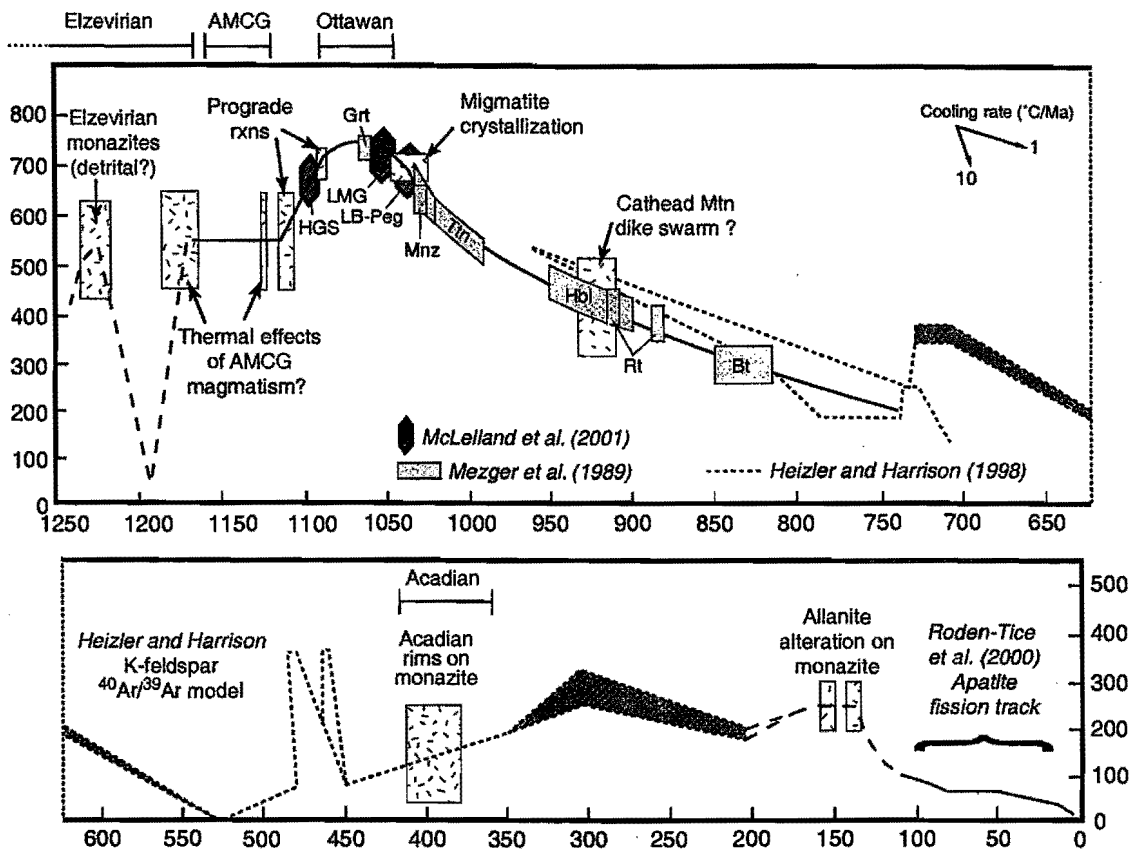


Figure 12. Temperature-time plot summarizing data from Mezger et al. (1989), McLelland et al. (2001; zircon shapes), Heizler and Harrison (1998; $^{40}\text{Ar}/^{39}\text{Ar}$), Roden-Tice et al. (2000; apatite fission track), and this study (boxes with the confetti pattern). Abbreviations are: HGS = Hawkeye Granite Suite, LB-Peg = Undeformed pegmatite from Lyonsdale Bridge Falls, LMG = Lyon Mountain Gneiss; mineral abbreviations include Bt = biotite, Grt = garnet, Hbl = hornblende, Mnz = monazite, Rt = rutile, Ttn = titanite (sphene).

growth during melt crystallization. The still younger age of 923 Ma probably represents monazite growth in association with pegmatite intrusions.

The Adirondacks were overlain unconformably by the Potsdam sandstone in the early Cambrian, so the temperature of the rocks must have been near surface temperatures. $^{40}\text{Ar}/^{39}\text{Ar}$ thermochronology (Heizler and Harrison, 1998) indicates a complex Paleozoic thermal history, with maximum temperatures reaching 400 °C. The temperature of allanite formation is not known, but it is probably between 200-300 °C. Fission track ages require a temperature of 100-120 °C at 120 Ma, suggesting that there may have been a pulse of rapid uplift in the middle Jurassic.

REFERENCES CITED

- Bohlen, S.R., Valley, J., and Essene, E., 1985, Metamorphism in the Adirondacks. I. Petrology, pressure, and temperature: *Journal of Petrology*, v. 26, p. 971-992.
- Heizler, M.T., and Harrison, T.M., 1998, The thermal history of the New York basement determined from $^{40}\text{Ar}/^{39}\text{Ar}$ K-feldspar studies: *Journal of Geophysical Research*, v. 103, no. B12, p. 29795-29814.
- Hodges, K.V., and Crowley, P.D., 1985, Error estimation and empirical geothermobarometry for pelitic systems: *American Mineralogist*, v. 70, p. 702-709.
- Kohn, M.J., and Spear, F.S., 2000, Retrograde net transfer reaction insurance for pressure-temperature estimates: *Geology*, v. 28, no. 12, p. 1127-1130.
- McLelland, J., Hamilton, M., Selleck, B., McLelland, J., Walker, D., and Orrell, S., 2001, Zircon U-Pb geochronology of the Ottawa Orogeny, Adirondack Highlands, New York: regional and tectonic implications: *Precambrian Research*, v. 109, p. 39-72.
- Mezger, K., Hanson, G.N., and Bohlen, S.R., 1989, High-precision U-Pb ages of metamorphic rutile: application to the cooling history of high-grade terranes: *Earth and Planetary Science Letters*, v. 96, p. 106-118.
- Mezger, K., Rawnsley, C., Bohlen, S., and Hanson, G., 1991, U-Pb garnet, sphene, monazite, and rutile ages: Implications for the duration of high grade metamorphism and cooling histories, Adirondack Mts., New York: *Journal of Geology*, v. 99, p. 415-428.
- Patino Douce, A. E., Johnston, A.D., and Rice, J.M., 1993, Octahedral excess mixing properties in biotite: A working model with applications to geobarometry and geothermometry: *American Mineralogist*, v. 78, p. 113-131.
- Roden-Tice, M.K., Tice, S.J., and Schofield, I.S., 2000, Evidence for differential unroofing in the Adirondack Mountains, New York State, determined by apatite fission-track thermochronology: *Journal of Geology*, v. 108, p. 155-169.
- Spear, F.S., and Kohn, M.J., 1996, Trace element zoning in garnet as a monitor of crustal melting: *Geology*, v. 24, p. 1099-1102.
- Spear, F.S., and Markussen, J.C., 1997, Mineral zoning, P-T-X-M phase relations, and metamorphic evolution of some Adirondack granulites, New York: *Journal of Petrology*, v. 38, no. 6, p. 757-783.
- Spear, F.S., and Parrish, R.R., 1996, Petrology and cooling rates of the Valhalla Complex, British Columbia, Canada: *Journal of Petrology*, v. 37, no. 4, p. 733-765.
- Valley, J., Bohlen, S.R.; Essene, E.J., and Lamb, W., 1990, Metamorphism in the Adirondacks. II. The role of fluids: *Journal of Petrology*, v. 31, pt. 3, p. 555-596.
- Whitney, P.R., 1978, The significance of garnet isograds in the granulite facies rocks of the Adirondacks: in *Metamorphism in the Canadian Shield*, Geol. Survey of Canada, Paper 78-10, p. 357-366.
- Wing, B.A., Ferry, J.M., and Harrison, T.M., 1999, The age of andalusite and kyanite isograds in New England from Th-Pb ion microprobe dating of monazite: *Geological Society of America Abstracts with Programs*, v. 31, p. A-40.

